Revisiting the Sunspot Number as EUV proxy for ionospheric F2 critical frequency

Bruno S. Zossi[1,2], Franco D. Medina[1,2], Trinidad Duran[3,4], Blas F. de Haro Barbas[1,2] and Ana G. Elias[1,2]

(1) Laboratorio de Ionosfera, Atmosfera Neutra y Magnetosfera (LIANM), Facultad de Ciencias Exactas y Tecnología (FACET), Universidad Nacional de Tucumán (UNT), Argentina

(2) INFINOA, CONICET-UNT, Argentina

(3) Departamento de Física, Universidad Nacional del Sur (UNS), Bahía Blanca, 8000, Argentina

(4) Instituto de Física del Sur (CONICET-UNS), Bahía Blanca, 8000, Argentina

Abstract:

This study reconsiders the Sunspot Number (Sn) as a solar extreme ultraviolet (EUV) proxy for modeling the ionospheric F2 layer's critical frequency (foF2) over the period 1960-2023. We compare the performance of Sn with F10.7 and F30 solar radio fluxes, focusing on their ability to model the Global Ionospheric index (IG). Our results reveal that while F30 has shown a better correlation in recent solar cycles, the Sn is the most stable and reliable over the entire dataset, obtaining the highest correlation. In addition, if we remove the saturation effects from the considering a maximum value of Sn, the correlation increases, outperforming all other proxies, and predicting correctly the long-term trend estimated by general circulation models.

Plain Language Summary

The Earth's ionosphere, a critical layer for radio communication and GPS signals, is influenced by the Sun's radiation. To understand how the ionosphere changes over time, scientists use measurements of solar activity called proxies. In this study, different proxies are evaluated to find the best one for modeling ionospheric conditions over the last 60 years. Despite being an older measure, we found that the Sunspot Number is the most reliable for long-term studies, outperforming newer proxies in some cases. Our work suggests that relying on newer proxies might lead to inaccurate predictions, especially during periods of low solar activity.

Key Points

- The Sunspot Number (Sn) outperforms F30 and F10.7 solar proxies in long-term ionospheric datasets, especially before 1980 and during recent solar cycles.
- Removing the saturation effect from the Sn dataset further enhances its correlation with the Global Ionospheric index (IG), improving long-term trend predictions.
- The study emphasizes the variable performance of solar proxies over time, with Sn showing the greatest stability for modeling ionospheric conditions across six decades.

1. Introduction:

The understanding of atmospheric trends became a critical area of study in the last century. Besides the troposphere, the upper atmosphere is also affected by human activities. Many modern technologies, such as long-distance telecommunications, global positioning systems (GPS), and satellite communications, rely on space and near-Earth physics (Zolesi and Cander, 2014). One important part of the upper atmosphere is the ionosphere, defined as the zone where the presence of free charges is high enough to affect the propagation of electromagnetic waves. Long-term trends in this region arise primarily from the greenhouse effect but are also influenced by long-term solar periodicities and the secular variation of Earth's magnetic field (Lastovicka, 2023).

This ionized area is mainly affected by solar extreme ultraviolet radiation (EUV), which is absorbed by the neutral components, heating and ionizing them. To model this atmospheric layer, direct measurements of EUV are needed. However, such data have only been available since the satellite era, therefore, several models were developed using EUV proxies, or, different measurements that are closely linked to the needed variable (Bilitza et al. 2022, Liu et al. 2010). Modern proxies measure solar irradiance at specific wavelengths in satellites, avoiding the interaction with the atmosphere. The most common are magnesium II wing-to-core ratio, helium II, and Lyman-alpha, among others.

The ionospheric structure has been measured since the 1930s after the development of the ionosonde. This instrument operates by emitting a vertical electromagnetic wave from the ground and waiting for the reflection of the wave. The internal layers are reached using different frequencies. The ionosphere is mainly studied through ionosonde databases, mainly due to their long period and the reliability of the available data. The main data produced by ionosondes are the critical frequencies and the peak height of each layer.

Over the past decades, various solar indices have been employed as proxies for estimating ionospheric parameters. Among these, the Sn has historically been one of the most reliable proxies due to its long record and strong correlation with solar EUV radiation, which directly affects the ionosphere. However, newer solar indices, such as the F10.7 cm solar radio flux (Lastovicka et al. 2006, Mielich and Bremer (2013), Jakowski et al. 2024), and the more recent F30 (Lastovicka 2021, Dudok de Wit and Bruinsma 2017, Zossi et al. 2024), as well as MgII (de Haro Barbas et al. 2021), have been introduced as alternatives that may offer better correlations under specific conditions or periods.

Recent studies have debated the effectiveness of these proxies, particularly in representing ionospheric trends during periods of low solar activity, such as the deep minima of solar cycles 24 and 25. These discussions have highlighted the need for continuous evaluation of solar proxies to ensure accurate long-term trend predictions, which are crucial for both scientific understanding and practical applications in space weather forecasting.

In recent years, some articles studied the changes in the relationship between the sunspot number and the solar radio fluxes, identifying a trend associated with the Sun that affects this relationship (Clette 2021, Mursula et al. 2022, 2024). The solar radio fluxes trend to increase compared to the sunspot number, this trend may introduce an error in models, which rely on these indices.

In this study, we assess the performance of the Sn, F10.7, and F30 as proxies for modeling ionospheric foF2 for the period 1960-2023, particularly focusing on their ability to model the ionospheric index IG, a key indicator of global ionospheric conditions. We examine the stability and correlation of these proxies over different solar cycles and discuss the implications of choosing one proxy over another for long-term ionospheric studies. This procedure results in a better performance of Sn over F10.7 and F30 to reproduce the complete IG dataset, mainly during the complicated solar cycles 20, 23, and 24.

2. Data

The foF2 monthly median time series used in this work are from the following 10 stations: Wakkanai (45.2°N, 141.4°E), Kokubunji (35.7°N, 139.5°E), Okinawa (26.3°N, 127.6°E), Hobart (42.5°S, 147.2°E), Canberra (35.2°S, 149.1°E), Townsville (19.2°S, 146.5°E), Sodankyla (67.3°N, 26.3°E), Boulder (40.1°N, 105.2°W), Juliusruh (54.6°N, 13.4°E), and Rome (41.5°N, 12.3°E). The selected stations have long records, covering, in some cases, more than 60 years. Due to the uncertainties and bad reading, some data were discarded. The criteria used to calculate the monthly medians for each hour required at least 15 days available with measurements in every month, and checking outliers in every case. Most of the datasets were extracted from Damboldt and Suessmann database (Damboldt and Suessman 2012). The data was updated until 2022 using records from Lowell GIRO Data Center (LGDC) (Reinisch and Galkin 2011). foF2 from the Digital Ionogram Data Base (DIDBase) at LGDC has a frequency of 5 to 15 minutes. To obtain the monthly medians, data with Autoscaling Confidence Score (CS) greater than 60% was first selected, and then the hourly median for each month was estimated. We checked that the last two years available from Damboldt and Suessman database had a reasonable coincidence (within 5%) with the data obtained from GIRO.

In this work, the Global Ionospheric index (IG) is used to analyze the solar proxies. IG was originally computed using 13 globally distributed ionosonde stations. The distribution of these stations was a compromise between good global coverage and reliable long-operating-period ionosonde stations. However, due to station closures and data unavailability, the number of stations used in IG has decreased to four (Brown et al., 2018). Therefore, since IG is derived from ionospheric measurements, it captures foF2 variations not driven solely by solar activity, such as those caused by increased greenhouse gases.

3. Methodology

In this work, we use linear regressions between the annual averaged IG index, which represents ionospheric foF2, and solar proxies. The linear regression is a simple statistical method that models the relation between two variables using a linear equation,

$$y = \alpha_0 + \alpha_1 x \quad (1)$$

where α parameters are the regression coefficients, usually estimated using least squares, and **x** and **y** are the independent and dependent variables, respectively.

This regression is widely used for systems highly sensitive to a given variable or parameter. For example, many upper atmosphere parameters, when dealing with annual means, respond to the solar flux almost linearly. We also extend to a second-order regression, which is the same procedure, but adding a squared term of variable x.

To compare the performance of each proxy we use the squared correlation coefficient, R^2, which provides a measure of the variance of y predicted by the model using the independent variables.

4. Results and Discussion

Using IG index as a global mean ionospheric condition. IG values are scaled to sunspot number, it represents foF2 from different stations around the world. Figure 1 shows the yearly averaged values of foF2 for the stations used in this work and the IG index, the correlation between both is also plotted. With an R^2 of 99.6%, we can say that the IG index is a reliable representation of ionospheric conditions. Therefore, we will use it to compare with the solar EUV proxies.

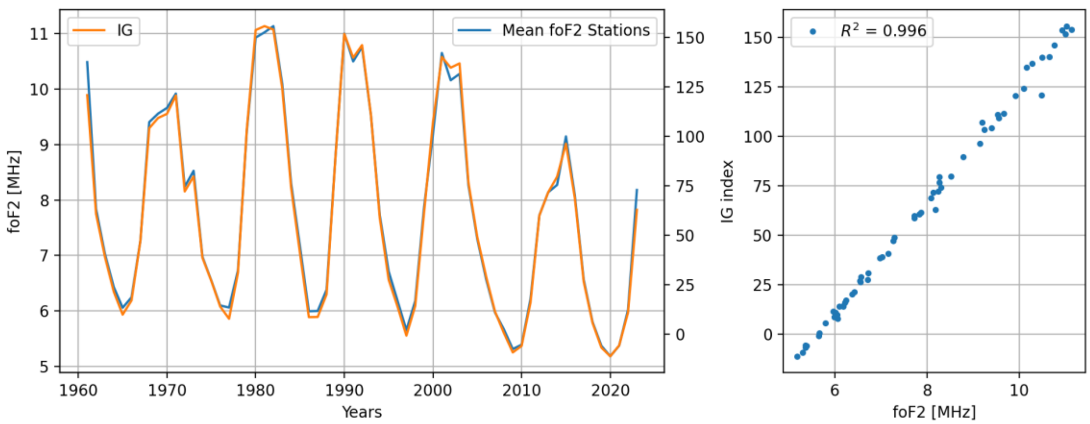

Figure 1. Yearly noon mean (12 LT) foF2 for the ten stations used in this work (blue), and IG index (orange). The right panel shows the linear correlation between IG and foF2, the explained variance R^2 = 0.996.

The variability of ionospheric foF2, at the interannual scale, is mainly driven by solar activity. For this reason, many (practically any) EUV proxies result in an excellent correlation with annual averaged foF2.

As we mentioned, in the last years, many articles have been published trying to find the correct proxy for long-term trend estimation. Historically, the more used were the oldest, the sunspot number, and the solar fluxes at radio wavelengths, having measured datasets of 70 years and more. However, such long datasets for ionospheric conditions are uncommon, just a bunch of measuring stations have reliable data in this period.

Lastovicka (2021) criteria for selecting the best solar proxy include the high correlation, temporal stability, and, the trend estimation having a consistent sign throughout the entire period. Based on these factors, the study concluded that F30 is the most suitable EUV proxy for ionospheric long-term trend estimation. The trend estimation is compared to general circulation models (Solomon et al. 2018), where the solar activity remains constant while greenhouse gases increase, resulting in a trend of ~-0.6 %/decade for foF2.

As the main issue is to find long ionospheric datasets, in many articles, the trends are often assessed using data up to 2008, avoiding the deep solar minimum, or from 1985 to the present. The important historical issues were the correlation decreasing in some periods and the change in the estimated trend after filtering the solar activity. These problems turn into the necessity of looking for other solar EUV proxies, particularly given the unique characteristics of the last solar cycles 24 and 25, which featured two deep minima with prolonged periods of zero sunspot numbers. During these deep minima, the ionospheric foF2 drops below historical minimum values, this fact can be easily noted since the IG index takes the most quantity of negative values in the last two cycles.

The stability of the correlation between proxies and data results in a slight average correlation of F30 over Sn and F10.7. This can be seen in Figure 2, where an 11-year centered moving correlation was calculated between IG and the three proxies. F10.7 shows two periods of lower correlation, this is a key reason for the need to use another proxy. On average, F30 has a higher correlation using this comparative analysis, especially in the last cycle, where correlations for the other proxies decrease. Sn has a step down in this last cycle but is the best from 1990 to 2008 approximately, where solar fluxes have a noticeable correlation decrease.

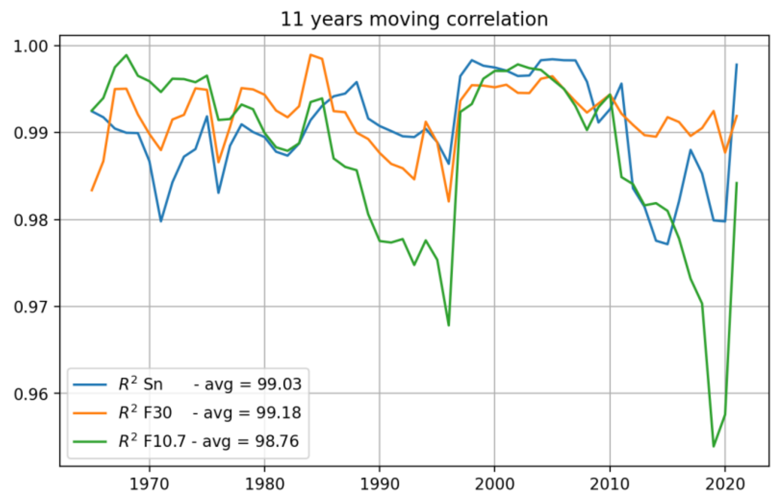

Figure 2. 11-year moving squared linear correlation between IG and solar EUV proxies: Sn (blue), F30 (orange), and F10.7 (green).

The linear correlation analysis indicates that Sn and F30 are better reproducing the variability of foF2, through the IG index. Figure 3 shows the IG values modeled linearly using both proxies along with the original dataset. This figure helps to contextualize the moving correlation seen in Figure 2. In all maximums after 1980, F30 is closer to IG values, however, in the complete previous solar cycle; Sn models better the ionospheric index. On the other hand, during minimum solar periods, Sn outperforms F30, even during the last two deep minimum cycles. Taking into account that Sn has a minimum possible value of zero, is expected to fail to reproduce these last two cycles, however, F30 does not reproduce the IG index decrease.

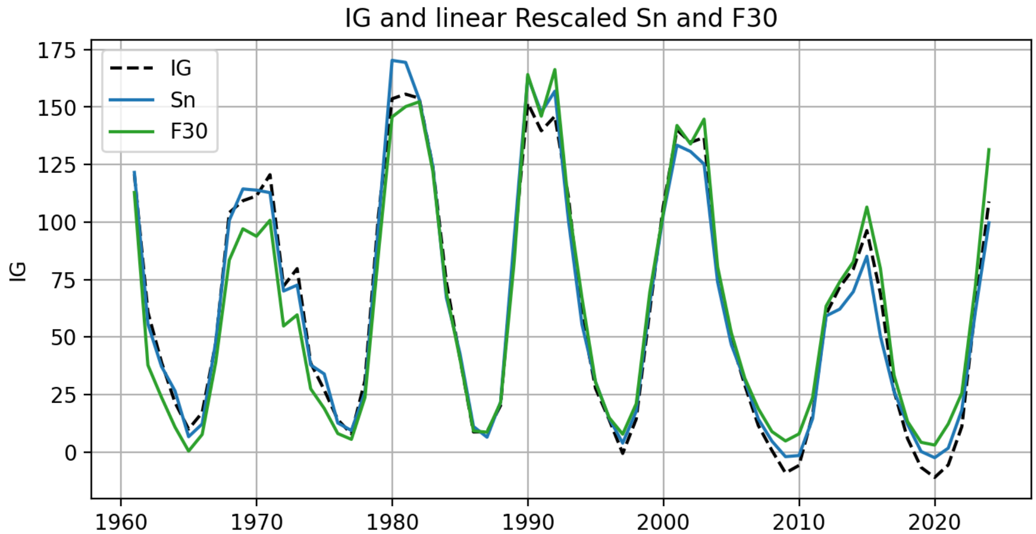

Figure 3. Linear modeling of the ionospheric IG index using F30 (green) and Sn (blue), with the observed IG index (black dashed line).

There is a clear trend between Sn and F30, note in Figure 3 how F30 (green line) is under the Sn (blue line) up to ~1990, where two lines cross, and after this time, F30 models higher values of IG at almost every point. This behavior is closely linked to the analysis made by Mursula et al. (2024); they compare the solar flux indices with the sunspot number, identifying this increasing trend.

At this point, an important problem arises, if solar fluxes increase compared to IG, which represents ionospheric foF2 level, we can anticipate a decreasing trend in the residuals if we subtract IG modeled with F30 from the original data. Perhaps, looking for a proxy with a decreasing trend led us to a mistake with F30, mainly, taking into account that F30 do not obtain the highest correlation before ~1980.

This can be noted in Figure 4, where we perform an ending point moving correlation, fixing the first year in 1960, changing the last year, and calculating the linear correlation of IG and the three proxies. Additionally, the same analysis is performed in reverse, fixing the final year at 2023, changing the first year, and estimating the linear correlation. In Figure 4, the superior performance of Sn to predict IG is clear, the left panel shows that starting the analysis in 1960, Sn is the best in almost the complete period, except for F10.7 at the beginning. On the other hand, the right panel explains why F30 is sometimes considered the best, fixing the last year and adding years backward in time, can be noted that, if the correlation analysis begins in the period 1980-1990, F30 is the best, but looking the complete panel, is clear that is just for that period. This is clearer comparing with Figure 3, where we noted that F30 fails to model the beginning and the end of the IG dataset. Moreover, Sn has a clear higher stability in this kind of analysis, therefore, the question is, why are we discarding Sn as a solar EUV proxy?

Note that the analysis of Figure 4 is completely different from the result of Figure 2, due to the variation in the initial and ending years, the result of the best correlation using F30 can be obtained reducing the period used in the correlation. This discrepancy is associated with the inclusion, or not, of solar cycle 20 (1964-1976), where F30 does not represent properly the IG index variability.

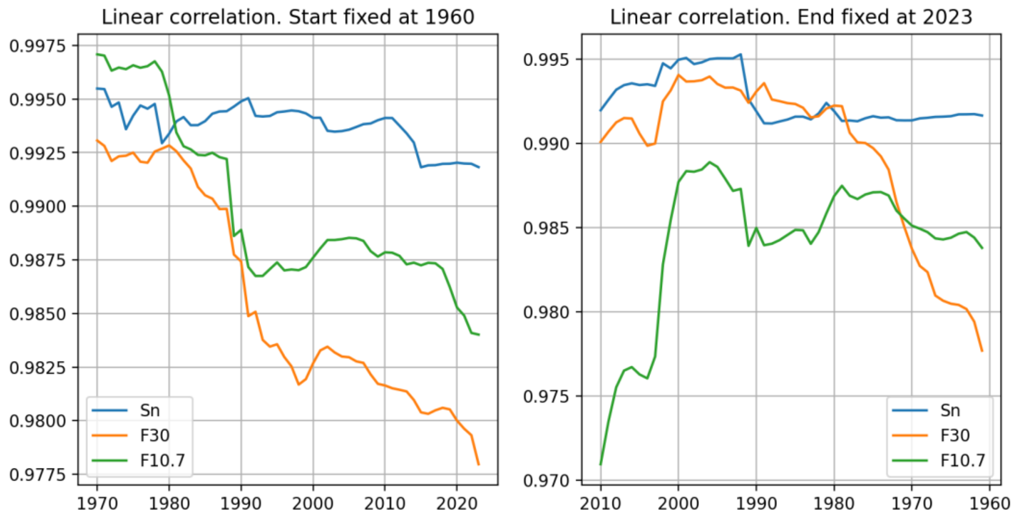

Figure 4. Squared linear correlation between IG and Sn, F30 and F10.7 with moving end year (left), and inverse, moving start year (right).

An important ionospheric feature is the saturation (Balan et al., 1994; Liu et al., 2003). During the daytime, there is a maximum possible value of foF2, even if solar flux continues increasing. This problem is more evident at shorter time scales. Many authors deal with this by performing a quadratic and even cubic regression between proxies and foF2 (Liu et al., 2006; Ma et al., 2009; Danilov and Berbeneva, 2023). However, this effect is not that clear when analyzing annual means. Figure 5 shows the linear and quadratic regression between proxies and IG separately for periods 1960-1997, and 1985-2023, to have the same number of years in each regression. Again, we can mention the higher performance of Sn in the first cycles, and F10.7 is the second-best proxy. In contrast, F30 obtains a higher correlation in the second period. There is a weak improvement using quadratic regression at the annual scale, this can be noticed in each panel. The F10.7 exhibits a more significant increase in the correlation.

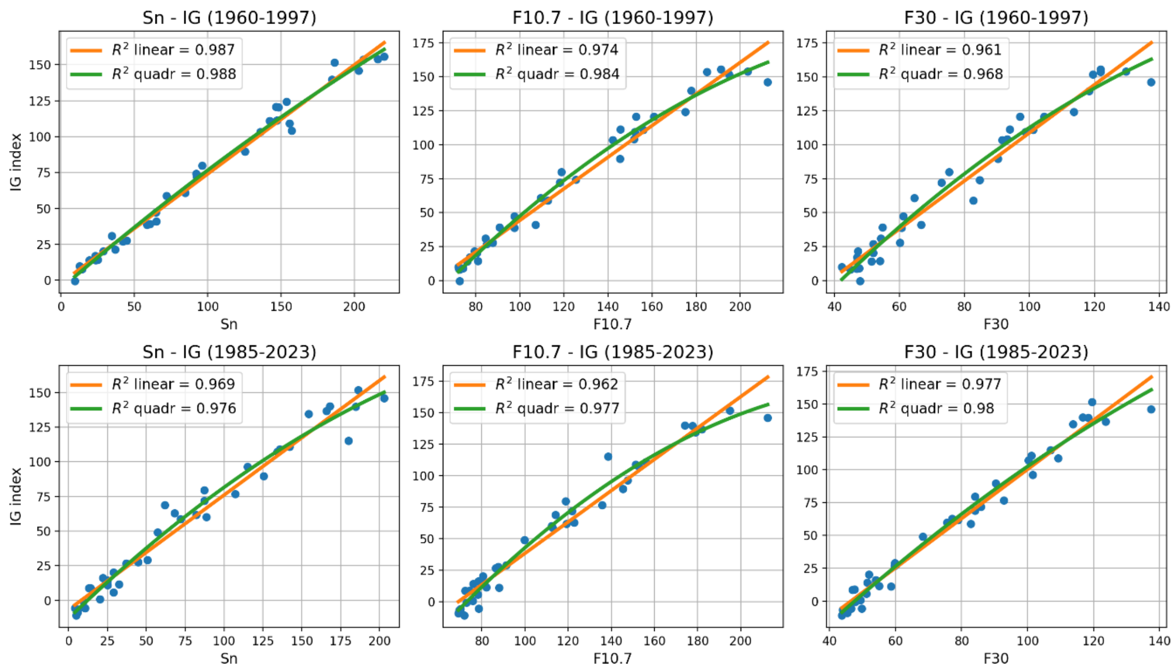

Figure 5. Linear and quadratic regression between proxies and IG separately for periods 1960-1997 (top panels), and 1985-2023 (bottom panels).

Is then the sunspot number the best EUV proxy to model foF2? The evidence up to this point suggests that is more stable considering longer datasets. The saturation effect could be affecting the correlation, therefore, subtracting from the daily dataset the Sn higher than 230 (~5% of data) and calculating the annual mean we obtain an excellent improvement in the linear correlation between Sn and IG. This method can be also used with F30 and F10.7, but the improvement is not as good as with the sunspot number (see Table 1). In addition, we model the annual IG using a quadratic regression; both results can be seen in Figure 6. Since Sn is the only proxy that shows the down step between cycle 23 and 24 minimums, like IG and most ionospheric stations, it obtains the highest correlation using the complete period.

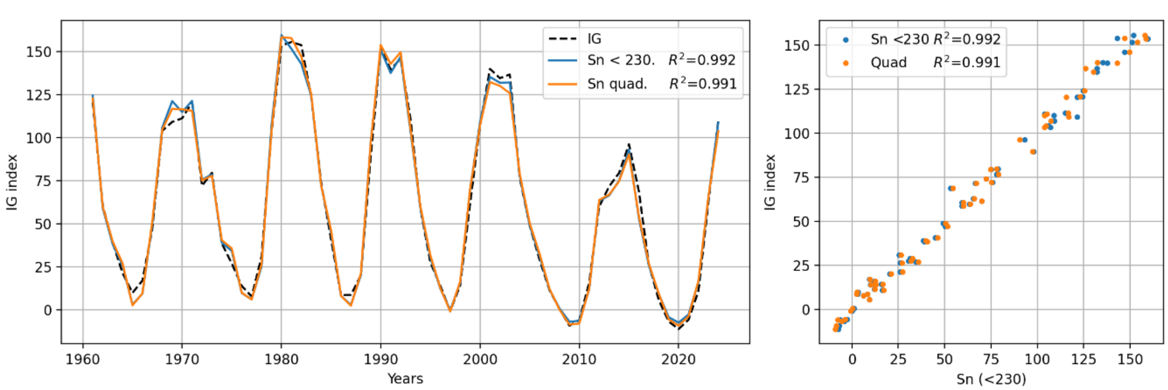

Figure 6. IG index (black dashed) and IG index modeled using quadratic regression (orange) and Sn de-saturated (<230, blue). The right panel shows IG vs IG modeled.

The correlation using a de-saturated Sn and quadratic regression shows a significant improvement over the original dataset, compared to Sn in Figure 3. The maximums of all cycles after 1970 are close to IG values. Moreover, the last two minimums are much better represented using the quadratic regression and de-saturating the Sn dataset. The squared correlations between indices and stations using quadratic regression can be seen in Table 1, compared to linear and de-saturated Sn. The Table shows that quadratic regression using Sn is, on average, the most effective to predict the ionospheric foF2, followed by Sn de-saturated and quadratic F10.7.

Table 1. Squared correlation (R^2) between stations and indices using a quadratic regression over the complete period (1960-2023), compared with linear and de-saturated Sn.

	Sn linear	F30 quad	F10.7 quad	Sn quad	Sn (<230)
Okinawa	0.917	0.859	0.940	0.944	0.939
Wakkanai	0.967	0.968	0.966	0.970	0.968
Kokubunji	0.981	0.979	0.984	0.989	0.988
Townsville	0.947	0.921	0.968	0.972	0.967
Canberra	0.980	0.972	0.983	0.988	0.989
Hobart	0.974	0.975	0.976	0.980	0.980
Juliusruh	0.983	0.981	0.978	0.984	0.981
Rome	0.970	0.971	0.976	0.979	0.978
Boulder	0.953	0.950	0.957	0.962	0.965
Sodankyla	0.911	0.900	0.901	0.911	0.907
Average	**0.958**	**0.947**	**0.963**	**0.968**	**0.966**

The only remaining task is the estimation of the long-term trend using a highly reliable proxy. From Figure 6, we can expect a nearly zero trend for the complete period. This is confirmed by filtering the solar activity from the IG dataset using de-saturated Sn and calculating the residuals, which yield a trend of -0.008 %/decade. However, if we take a close look at the minimum's solar times in Figure 6, a clear trend can be noted: IG is higher than Sn in 1965 but lower in 2020. Considering that the CO2 cooling effect over the thermosphere is more pronounced during minimum solar conditions (Emmert et al. 2008, Brown et al. 2024), we could assume a more noticeable effect over the ionospheric parameters as well during lower solar conditions. The theoretical trend estimated using a general circulation model (WACCM-X) is -0.6 %/decade for foF2 (Solomon et al. 2018). Therefore, by focusing on the minimum solar years (1963-1965, 1975-1977, 1985-1987, 1995-1997, 2007-2009, 2018-2020), the trend results in -0.79 %/decade, really close to the theoretical value. The residuals from this procedure are shown in Figure 7, where a clear and constant trend is noticed. Is important to note that experimental trend using a similar approach on ionospheric stations data results in much higher values, between 0.04 and 0.21 MHz/decade (Lastovicka 2024; Zossi et al. 2024). Mikhailov et al. (2017) also found a better correlation using the sunspot number over F10.7 in the long-term trend of critical frequency of E-layer.

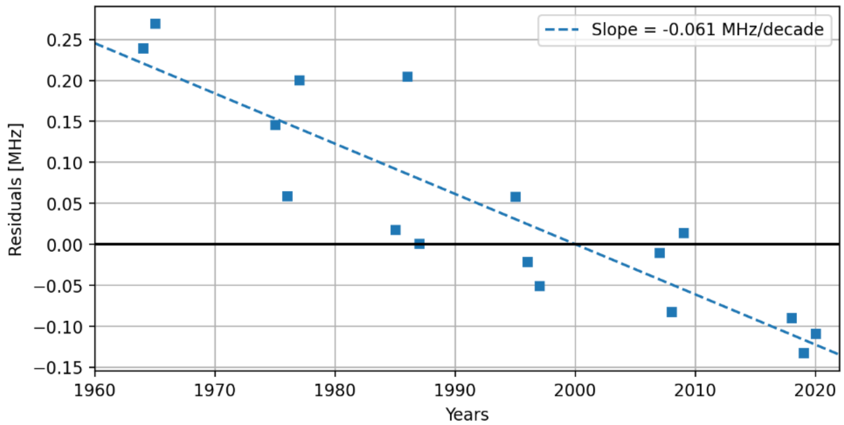

Figure 7. Residuals for solar cycle minimums years using Sn de-saturated.

5. Conclusions

In this work, we found that the sunspot number is the most reliable solar EUV proxy for predicting ionospheric index IG over the period 1960-2023. This index is a good indicator of the global ionospheric foF2, as is shown in Figure 1, and supporting by the R^2 value.

While many recent articles claim F30 as the superior solar EUV proxy, it fails at representing the step down during the last two solar minimums—a decline that is evident in the Sn dataset. Some of these studies analyze shorter periods in order to use more stations. In Figure 2, we show that F30 is the proxy with better stability to represent each cycle separately. However, analyzing the period 1960-2023, Sn outperforms the F30 correlation, as shown in Figure 3.

The main issue with F10.7 and F30 is the last two solar cycle minimums, where the ionospheric foF2 decreases more than expected, and a linear model cannot reproduce this decrease using the solar radio fluxes. The sunspot number, on the other hand, effectively handles this issue. When applying a quadratic regression, or neglecting saturation effects from the daily database, Sn obtains the highest correlation, reproducing reliably the last two cycles.

The only problem with this methodology is that if we calculate the long-term trend filtering the solar activity, we do not obtain the trend predicted by the global circulation models. Nevertheless, as we point out in Figure 6, minimum solar activity periods have a noticeable trend that results to be in good agreement with the theoretical trend.

Acknowledgment

B.S. Zossi, F.D. Medina, and A.G. Elias acknowledge research projects PIP 2957 and PIUNT E756. T. Duran acknowledges research projects PICT 2019-03491 and PGI 24/F083.

Open Research

All data used in this work are in public domain. For ionospheric foF2 (1) National Institute of Information and Communications Technology, NICT (https://wdc.nict.go.jp/IONO/HP2009/ISDJ/manual_txt-E.html). (2) The Australian Bureau of Meteorology (https://downloads.sws.bom.gov.au/wdc/iondata/au/). (3) The Lowell GIRO Data Center (https://giro.uml.edu/didbase/scaled.php). F10.7 at https://spaceweather.gc.ca/forecast-prevision/solar-solaire/solarflux/sx-en.php. Sn from the revised Sn database obtained from SILSO (Sunspot Index and Long-term Solar Observations), Royal Observatory of Belgium, at https://www.sidc.be/SILSO/datafiles, F30 from the National Astronomical Observatory of Japan at http://solar.nro.nao.ac.jp/norp/html/daily_flux.html.

References

Balan, N., Bailey, G. J., & Moffett, R. J. (1994). Modeling studies of ionospheric variations during an intense solar cycle. *Journal of Geophysical Research: Space Physics*, *99*(A9), 17467–17475. https://doi.org/10.1029/94JA01262

Bilitza, D., Pezzopane, M., Truhlik, V., Altadill, D., Reinisch, B. W., & Pignalberi, A. (2022). The International Reference Ionosphere Model: A Review and Description of an Ionospheric Benchmark. *Reviews of Geophysics*, *60*(4), e2022RG000792. https://doi.org/10.1029/2022RG000792

Brown, M. K., Lewis, H. G., Kavanagh, A. J., Cnossen, I., & Elvidge, S. (2024). Future Climate Change in the Thermosphere Under Varying Solar Activity Conditions. *Journal of Geophysical Research: Space Physics*, *129*(9), e2024JA032659. https://doi.org/10.1029/2024JA032659

Clette, F. (2021). Is the F10.7cm – Sunspot Number relation linear and stable? *Journal of Space Weather and Space Climate*, *11*, 2. https://doi.org/10.1051/SWSC/2020071

Damboldt T, Suessmann P (2012). Consolidated Database of Worldwide Measured Monthly Medians of Ionospheric Characteristics foF2 and M(3000)F2. INAG (Ionosonde Network Advisory Group) Bulletin 73 https://www.ursi.org/files/Commission-Websites/INAG/web-73/2012/damboldt_consolidated_database.pdf

Danilov, A. D., Berbeneva, N. A., & Konstantinova, A. V. (2024). Trends in the F2-layer parameters to 2023. *Advances in Space Research*, *73*(12), 6054–6065. https://doi.org/10.1016/J.ASR.2024.03.036

Danilov, A. and Berbeneva, N. (2023). Statistical analysis of the critical frequency foF2 dependence on various solar activity indices, *Advances in Space Research*.

de Haro Barbás, B. F., Elias, A. G., Venchiarutti, J. V., Fagre, M., Zossi, B. S., Tan Jun, G., & Medina, F. D. (2021). MgII as a Solar Proxy to Filter F2-Region Ionospheric Parameters. *Pure and Applied Geophysics*, *178*(11), 4605–4618. https://doi.org/10.1007/S00024-021-02884-Y

Dudok De Wit, T., & Bruinsma, S. (2017). The 30 cm radio flux as a solar proxy for thermosphere density modelling. *Journal of Space Weather and Space Climate*, *7*, A9. https://doi.org/10.1051/SWSC/2017008

Emmert, J. T., Picone, J. M., & Meier, R. R. (2008). Thermospheric global average density trends, 1967–2007, derived from orbits of 5000 near-Earth objects. *Geophysical Research Letters*, *35*(5), 5101. https://doi.org/10.1029/2007GL032809

Jakowski, N., Hoque, M. M., & Mielich, J. (2024). Long-term relationships of ionospheric electron density with solar activity. *Journal of Space Weather and Space Climate, 14,* 24. https://doi.org/10.1051/SWSC/2024023

Laštovička, J., Mikhailov, A. V., Ulich, T., Bremer, J., Elias, A. G., Ortiz de Adler, N., Jara, V., Abarca del Rio, R., Foppiano, A. J., Ovalle, E., & Danilov, A. D. (2006). Long-term trends in foF2: A comparison of various methods. *Journal of Atmospheric and Solar-Terrestrial Physics*, *68*(17), 1854–1870. https://doi.org/10.1016/J.JASTP.2006.02.009

Laštovička, J. (2021). The best solar activity proxy for long-term ionospheric investigations. *Advances in Space Research*, *68*(6), 2354–2360. https://doi.org/10.1016/J.ASR.2021.06.032

Laštovička, J. (2023). Progress in investigating long-term trends in the mesosphere, thermosphere, and ionosphere. *Atmospheric Chemistry and Physics*, *23*(10), 5783–5800. https://doi.org/10.5194/ACP-23-5783-2023.

Laštovička, J. (2024). Dependence of long-term trends in foF2 at middle latitudes on different solar activity proxies. Advances in Space Research. https://doi.org/10.1016/J.ASR.2023.09.047.

Liu, H. L., Foster, B. T., Hagan, M. E., McInerney, J. M., Maute, A., Qian, L., Richmond, A. D., Roble, R. G., Solomon, S. C., Garcia, R. R., Kinnison, D., Marsh, D. R., Smith, A. K., Richter, J., Sassi, F., & Oberheide, J. (2010). Thermosphere extension of the Whole Atmosphere Community Climate Model. *Journal of Geophysical Research: Space Physics*, *115*(A12), 12302. https://doi.org/10.1029/2010JA015586

Liu, L., Wan, W., Ning, B., Pirog, O., and Kurkin, V. (2006). Solar activity variations of the ionospheric peak electron density, *Journal of Geophysical Research: Space Physics*, 111.

Liu, J. Y., Chen, V. I., & Lin, J. S. (2003). Statistical investigation of the saturation effect in the ionospheric foF2 versus sunspot, solar radio noise, and solar EUV radiation. *Journal of Geophysical Research: Space Physics*, *108*(A2), 1067. https://doi.org/10.1029/2001JA007543

Ma, R., Xu, J., Wang, W., & Yuan, W. (2009). Seasonal and latitudinal differences of the saturation effect between ionospheric NmF2 and solar activity indices. *Journal of Geophysical Research: Space Physics*, *114*(A10), 10303. https://doi.org/10.1029/2009JA014353

Mikhailov, A. V., Perrone, L., & Nusinov, A. A. (2017). A mechanism of midlatitude noontime foE long-term variations inferred from European observations. *Journal of Geophysical Research: Space Physics, 122*(4), 4466–4473. https://doi.org/10.1002/2017JA023909

Mielich, J., & Bremer, J. (2013). Long-term trends in the ionospheric F2 region with different solar activity indices. *Annales Geophysicae*, *31*(2), 291–303. https://doi.org/10.5194/ANGEO-31-291-2013

Mursula, K., Qvick, T., Holappa, L., & Asikainen, T. (2022). Magnetic Storms During the Space Age: Occurrence and Relation to Varying Solar Activity. *Journal of Geophysical Research: Space Physics*, *127*(12), e2022JA030830. https://doi.org/10.1029/2022JA030830

Mursula, K., Pevtsov, A. A., Asikainen, T., Tähtinen, I., & Yeates, A. R. (2024). Transition to a weaker Sun: Changes in the solar atmosphere during the decay of the Modern Maximum. *Astronomy & Astrophysics*, *685*, A170. https://doi.org/10.1051/0004-6361/202449231

Reinisch, B.W., Galkin, I.A, (2011). Global Ionospheric Radio Observatory (GIRO). Earth Planet Sp 63, 377–381. https://doi.org/10.5047/eps.2011.03.001

Solomon, S. C., Liu, H. L., Marsh, D. R., McInerney, J. M., Qian, L., & Vitt, F. M. (2018). Whole Atmosphere Simulation of Anthropogenic Climate Change. *Geophysical Research Letters*, *45*(3), 1567–1576. https://doi.org/10.1002/2017GL076950

Zolesi, B., & Cander, L. R. (2014). Ionospheric prediction and forecasting. *Ionospheric Prediction and Forecasting*, 1–240. https://doi.org/10.1007/978-3-642-38430-1

Zossi, B. S., Medina, F. D., Duran, T., & Elias, A. G. (2024). Selecting the best solar EUV proxy for long-term timescale applications. *Advances in Space Research*. https://doi.org/10.1016/J.ASR.2024.07.023